sustainability

MDPI

Article

Spatial Analysis of Air Pollutants in an Industrial City Using GIS-Based Techniques: A Case Study of Pavlodar, Kazakhstan

Ruslan Safarov [1], Zhanat Shomanova [2,*], Yuriy Nossenko [2,*], Eldar Kopishev [1], Zhuldyz Bexeitova [3] and Ruslan Kamatov [4]

[1] Department of Chemistry, Faculty of Natural Sciences, L.N. Gumilyov Eurasian National University, Astana 010000, Kazakhstan; safarov_rz@enu.kz (R.S.); kopishev_eye@enu.kz (E.K.)
[2] Higher School of Natural Science, Margulan University, Pavlodar 140002, Kazakhstan
[3] Eurasian Center for Innovative Development, Astana 010000, Kazakhstan; bb-zhuldyz@yandex.ru
[4] Department of Science, L.N. Gumilyov Eurasian National University, Astana 010000, Kazakhstan; krm305@mail.ru
* Correspondence: zshoman@yandex.ru (Z.S.); nosenko1980@yandex.ru (Y.N.)

Abstract: The given research employs high-resolution air quality monitoring and contemporary statistical methods to address gaps in understanding the urban air pollution in Pavlodar, a city with a significant industrial presence and promising touristic potential. Using mobile air quality sensors for detailed spatial data collection, the research aims to quantify concentrations of particulate matter ($PM_{2.5}$, PM_{10}), carbon monoxide (CO), nitrogen dioxide (NO_2), sulfur dioxide (SO_2), and ground-level ozone (O_3); assess their distribution; and identify key influencing factors. In this study, we employed Geographic Information Systems (GISs) for spatial analysis, integrating multi-level B-spline interpolation to model spatial variability. Correlation analysis and structural equation modeling were utilized to explore the relationships between variables, while regression analysis was conducted to quantify these relationships. These techniques were crucial for accurately mapping and interpreting spatial patterns and their underlying factors. The study identifies $PM_{2.5}$ and NO_2 as the primary contributors to air pollution in Pavlodar, with NO_2 exceeding the 24 h threshold in 87.38% of locations and $PM_{2.5}$ showing the highest individual air quality index (AQI) in 75.7% of cases. Correlation analysis reveals a positive association between $PM_{2.5}$ and AQI and a negative correlation between NO_2 and AQI, likely due to the dominant influence of $PM_{2.5}$ in AQI calculations. Structural equation modeling (SEM) further underscores $PM_{2.5}$ as the most significant impactor on AQI, while NO_2 shows no significant direct impact. Humidity is positively correlated with AQI, though this relationship is context-specific to seasonal patterns observed in May. The sectoral analysis of landscape indices reveals weak correlations between the green space ratio (GSR) and air quality, indicating that while vegetation reduces pollutants, its impact is minimal due to urban planting density. The road ratio (RR) lacks sufficient statistical evidence to draw conclusions about its effect on air quality, possibly due to the methodology used. Spatial variability in pollutant concentrations is evident, with increasing $PM_{2.5}$, PM_{10}, and AQI towards the east-northeast, likely influenced by industrial activities and prevailing wind patterns. In contrast, NO_2 pollution does not show a clear geographic pattern, indicating vehicular emissions as its primary source. Spatial interpolation highlights pollution hotspots near industrial zones, posing health risks to vulnerable populations. While the city's overall AQI is considered "moderate", the study highlights the necessity of implementing measures to improve air quality in Pavlodar. This will not only enhance the city's attractiveness to tourists but also support its sustainable development as an industrial center.

Keywords: air pollution; air quality index (AQI); particulate matter ($PM_{2.5}$; PM_{10}); green space ratio; road ratio; Pavlodar, Kazakhstan

Citation: Safarov, R.; Shomanova, Z.; Nossenko, Y.; Kopishev, E.; Bexeitova, Z.; Kamatov, R. Spatial Analysis of Air Pollutants in an Industrial City Using GIS-Based Techniques: A Case Study of Pavlodar, Kazakhstan. *Sustainability* **2024**, *16*, 7834. https://doi.org/10.3390/su16177834

Academic Editors: Jan A. Wendt, Kulyash Kaimuldinova and Zharas Berdenov

Received: 11 August 2024
Revised: 4 September 2024
Accepted: 6 September 2024
Published: 9 September 2024

1. Introduction

Air pollution is a critical environmental issue with far-reaching impacts on human health, ecosystems, and climate change. According to World Health Organization (WHO) [1], air pollution emerged as a significant health threat in 2019, contributing to approximately 6.7 million fatalities. Notably, noncommunicable diseases (NCDs) accounted for nearly 85% of these deaths. The range of affected NCDs included ischemic heart disease, stroke, lung cancer, asthma, chronic obstructive pulmonary disease (COPD), and diabetes. These statistics position air pollution as the second most prevalent cause of NCDs worldwide, surpassed only by tobacco use.

Urban areas, in particular, face significant challenges due to high concentrations of pollutants resulting from industrial activities, vehicular emissions, and other anthropogenic sources. Monitoring and managing air quality in cities is essential for safeguarding public health and ensuring sustainable urban development [2,3]. The necessity of studying the ecological state of the atmosphere for planning sustainable cities is emphasized in the works of Menconi et al., Wang et al., Zaini et al., and many others [4–6].

The city of Pavlodar in Kazakhstan is a prime example of where industrial emissions significantly contribute to air quality degradation. According to the statistical collection of the Ministry of Health of the Republic of Kazakhstan for 2020 [7], the number of cases of cancer in the Pavlodar region increased from 1111.1 to 1265.7 cases per 100 thousand people living. The number of oncological diseases in Pavlodar region is growing. So, in 2019, the Pavlodar region was in fourth place, and in 2020 it moved to first place in this indicator.

Tourism, as a growing industry, increasingly depends on the environmental quality of urban areas, especially in industrial cities where pollution levels can significantly influence the attractiveness of the destination [8]. In cities like Pavlodar, where industrial activities are prevalent, understanding the spatial distribution of air pollutants is critical not only for public health but also for the sustainable development of tourism infrastructure.

Previous studies have highlighted the adverse health effects associated with exposure to air pollutants such as particulate matter ($PM_{2.5}$ and PM_{10}), carbon monoxide (CO), sulfur dioxide (SO_2), nitrogen dioxide (NO_2), and ground-level ozone (O_3) [9]. These pollutants are known to cause respiratory and cardiovascular diseases, and long-term exposure can lead to severe health outcomes, including premature death [10]. However, there is a gap in localized, high-resolution studies that integrate comprehensive air quality monitoring with advanced statistical and spatial analysis techniques. Many studies on urban air pollution rely on data from a limited number of fixed monitoring stations, which do not provide sufficient spatial resolution to capture local variations in pollutant concentrations. This limitation hampers the ability to identify specific areas within a city that may experience higher levels of pollution. In Kazakhstan, the problem of studying the spread of air pollutants has been poorly studied [11–14]. Basically, periodic fluctuations in the level of pollution are studied. The spatial distribution and mapping of pollutants were not carried out. At the same time, such information should be studied and updated regularly. Previous research often focuses on individual pollutants or specific environmental factors without considering the complex interplay between multiple pollutants and environmental variables [15]. There is a lack of studies that integrate various data sources and analytical methods to provide a holistic view of air quality dynamics. Finally, most existing studies are conducted in cities with different industrial profiles and climatic conditions from Pavlodar. There is a dearth of research specifically tailored to the unique industrial and environmental context of Pavlodar, which includes significant contributions from petrochemical, aluminum, and other heavy industries.

This study employs high-resolution air quality monitoring and advanced statistical methods to address gaps in understanding urban air pollution in Pavlodar, a city with a significant industrial presence. Using mobile air quality sensors for detailed spatial data collection, the research aims to quantify pollutant concentrations, assess their distribution, and identify key influencing factors. Advanced analytical techniques, including correlation analysis, structural equation modeling, and multilevel B-spline interpolation, enable a comprehensive examination of relationships between pollutants and environmental variables.

It is hypothesized that in the industrial city, the spatial distribution of air pollutants is significantly influenced by both industrial emissions (not only from technological processes but also from dust, trucks, and building sites) and landscape characteristics like greening and roads. Specific areas may experience higher concentrations due to the complex interplay between these factors. Advanced spatial and statistical analyses reveal significant correlations between air quality indicators and environmental conditions, providing a detailed understanding of pollution dynamics that is essential for targeted measures and sustainable urban development.

This localized approach provides insights directly applicable to cities with similar industrial profiles, contributing to the broader field of urban air quality management. The resulting detailed understanding of pollution sources and their interactions with environmental variables is crucial for developing targeted interventions and policies to improve air quality and protect public health in industrial urban settings. Moreover, this study's findings are essential for enhancing the tourism potential of industrial cities by promoting sustainable urban development practices.

2. Materials and Methods

2.1. Research Area

The Pavlodar region is one of the largest economically developed regions of Kazakhstan. A diversified industrial complex has developed in the territory of the region [16]. The economic specialization of the region is metallurgy (production of aluminum and ferroalloys), power engineering, petrochemical industry, machine building, and mining. The industrial potential of the region is determined by large export-oriented industrial enterprises [17]. The main city of the Pavlodar region, Pavlodar, is one of the largest industrial centers of Kazakhstan, and the city has several major industrial zones: the Northern Industrial Zone located on the northern side of the city and the Central and Eastern Industrial Zones located on the eastern side [18].

The industrial zones of Pavlodar have a significant impact on the local economy, creating thousands of jobs and reducing unemployment. Furthermore, the presence of these zones attracts domestic and foreign investment, which contributes to economic growth and the modernization of production facilities. Many enterprises in these industrial zones implement modern technologies to minimize the environmental impact, which contributes to the improvement of the environmental situation in the city and the region [19].

The study area encompasses the residential sector of Pavlodar city, 28 square kilometers in total. The boundaries of the study area are illustrated in Figure 1. The research area used in this study covers an extent defined by the following coordinates: 8,562,113, 6,843,819 (minimum X, minimum Y), and 8,574,562, 6,856,769 (maximum X, maximum Y). This extent delineates the specific area of interest, ensuring that all spatial analyses and data manipulations are confined within these geographic boundaries. The coordinate values are presented in the EPSG:3857-WGS 84/Pseudo-Mercator, which was chosen to maintain consistency and accuracy in spatial data processing.

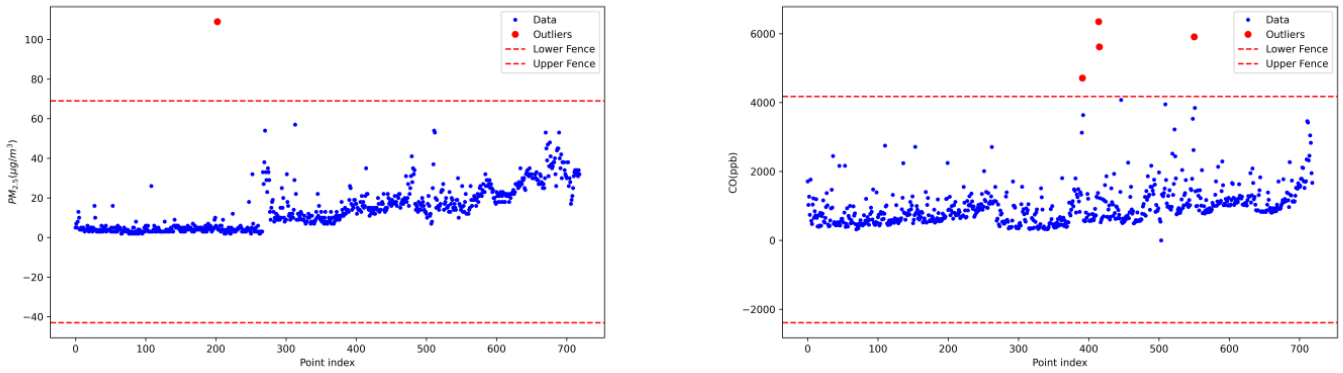

(**a**) (**b**)

Figure 1. Detection of outliers using graphical IQR method on examples of scatter plots for $PM_{2.5}$ (**a**) and CO (**b**).

2.2. Data Collection

Concentrations for pollutants $PM_{2.5}$, PM_{10}, CO, NO_2, SO_2, and O_3 as well as air temperature and relative humidity were obtained in the study area at 762 points. Data collection was performed in two sessions: from 9 A.M. to 9 P.M. on 19 May 2024 and from 9 A.M. to 1 P.M. on 20 May 2024. The standard interval between measurements was 1 min. Measurement was performed automatically with a mobile unit using an AQS008A air quality sensor (Sichuan Weinasa Technology Co., Ltd., The International Creative Federation Cross-Border E-Commerce Industry Park, Mianyang, China). The main specifications of the AQS008A sensor are presented in Table 1. The detection principles employed are laser measurement for $PM_{2.5}$ and PM_{10}, and electrochemical sensors for CO, SO_2, NO_2, and O_3. Obtained data were collected with Meteorological data logger AWS00X (Sichuan Weinasa Technology Co., Ltd., The International Creative Federation Cross-Border E-Commerce Industry Park, Mianyang, China).

Table 1. Specifications of air quality sensor AQS008A.

Monitoring Parameter	Measuring Range	Resolution	Accuracy
$PM_{2.5}$	0–1000 $\mu g/m^3$	1 $\mu g/m^3$	$\pm(10 \pm 10\%)$ (<500 $\mu g/m^3$) *
PM_{10}	0–1000 $\mu g/m^3$	1 $\mu g/m^3$	$\pm(10 \pm 10\%)$ (<500 $\mu g/m^3$)
Carbon monoxide	0–10 ppm	≤10 ppb	±5%F.S. **
Sulfur dioxide	0–5000 ppb	≤10 ppb	±5%F.S.
Nitrogen dioxide	0–5000 ppb	≤10 ppb	±5%F.S.
Ozone	0–5000 ppb	≤10 ppb	±5%F.S.
Temperature	−40–85 °C	0.1 °C	±0.3 °C (25 °C)
Humidity	0–100%RH	0.1%	±3%RH (10–80%RH when no condensation)

* The accuracy for PM2.5 and PM10 is specified as ±10 $\mu g/m^3$ with an additional uncertainty of ±10% of the measured value for concentrations below 500 $\mu g/m^3$. This means that for measurements under 500 $\mu g/m^3$, the total possible error includes a fixed error of ±10 $\mu g/m^3$ plus an additional variable error of ± 10% of the actual reading. ** F.S. (full scale) indicates that the specified accuracy of ±5% applies to the full scale of the measuring instrument. For example, if the instrument has a full scale of 100 units, the possible error is ±5 units, regardless of the current measurement value.

During the study, data outliers were identified in an initial sample of 762 measurements. As an essential part of data validation, the finding of outliers was conducted. Identifying and addressing outliers helped us to improve the quality and accuracy of data analysis, leading to more reliable and meaningful insights. The interquartile range (IQR) method was used to identify outliers in the data. During data analysis, the first (Q1) and third (Q3) quartiles were calculated for each column of data. The interquartile range (IQR) was defined as the difference between Q3 and Q1. The lower and upper limits were defined as Q1 − k × IQR and Q3 + k × IQR. The k value, which determines the threshold

for outlier detection, was selected using a graphical method tailored to each pollutant's distribution characteristics. For $PM_{2.5}$, PM_{10}, NO_2, and O_3, a k value of 3 was chosen, while for CO and SO_2, a higher k value of 5 was used. This differentiation was based on visual analysis of scatter plots for each pollutant, where data points were plotted against their ID (representing the relative time of measurement).

In the case of $PM_{2.5}$ (Figure 1a), a k value of 3 effectively identified extreme values without excluding too many data points that followed the overall trend. This can be seen by the position of the upper and lower fences (red dashed lines), which capture most of the data variation while still identifying clear outliers.

For CO (Figure 1b), a higher k value of 5 was necessary due to the greater natural variability observed in the data. The wider range between the upper and lower fences accommodates this variability, ensuring that only the most extreme points (well separated from the main data cluster) are classified as outliers.

This graphical approach allowed for a balance between sensitivity to true outliers and robustness against false positives, accounting for the unique distribution patterns of each pollutant. The selected k values effectively isolate unusual spikes or dips in concentration levels while preserving the overall trend and variability of the data. Thus, all points outside these thresholds were categorized as statistical outliers and removed from the dataset.

Thus, after applying data processing and cleaning techniques, the sample was reduced to 713 measurements, improving the accuracy and reliability of the subsequent analysis. The obtained dataset points are presented in Figure 2.

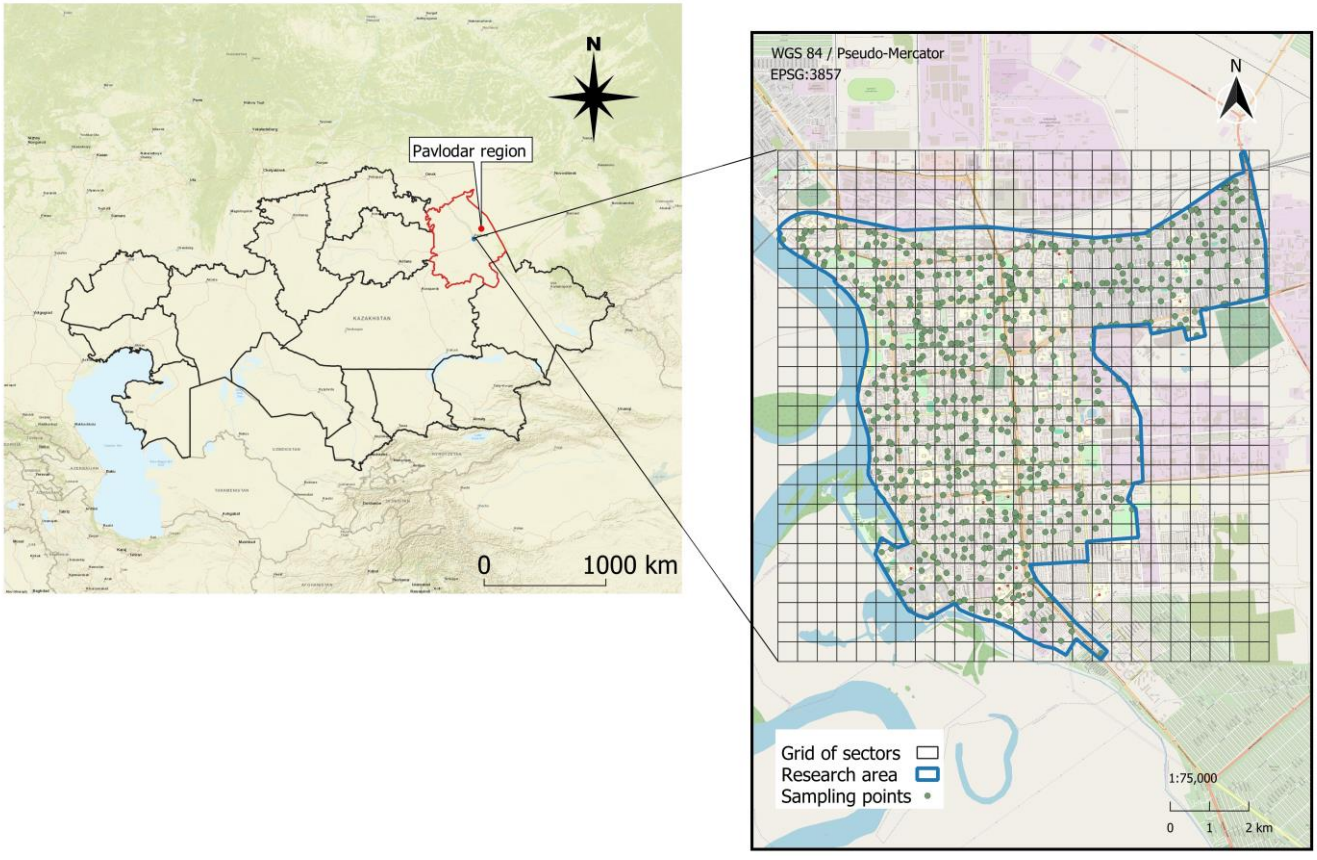

Figure 2. Map of Pavlodar city with research area and sampling points.

To facilitate a comprehensive and systematic analysis, the scope of the study area was divided into 650 sectors of 0.09 km^2 each, so each sector represents a square unit of the grid. Nevertheless, the sectoral analysis was performed for only 347 sectors lying within or adjoining the borders of the research area. This methodological approach allows for a more detailed examination of spatial variations and ensures that different parts of the city

can be studied in a structured manner. The landscape indicators were calculated for the sectors that intersect or lie within the boundaries of the research area. The grid of sectors is presented in Figure 2.

2.3. Landscape Indicators

2.3.1. Green Space Ratio (GSR)

Urban green spaces were defined as any land that is partly or completely covered with vegetation, such as parks, community, allotment or residential gardens, urban forests, or street trees [20]. For calculation and analysis, GSR was defined as a relation of Total Green Space Area to Total Land Area (1), where Total Green Space Area is the combined area of all greenery within the defined area, including trees and bushes and Total Land Area refers to the entire area being assessed, including both developed and undeveloped land. The formula for calculating the GSR is

$$GSR = \frac{Total\ Green\ Space\ Area}{Total\ Land\ Area} \times 100 \quad (1)$$

The detection of trees and shrubs was performed using a convolutional neural network YOLO8 (abbreviation from You Only Look Once, 8th version). YOLO8 is a state-of-the-art deep learning model designed for the rapid and precise detection of objects within images. The model exhibits high performance and is capable of efficiently processing images in real time, rendering it an optimal tool for segmentation and object classification tasks on satellite and aerial images [21].

The YOLO8 neural network was trained on available Maxar orthophotos captured in July 2022, which were segmented according to the sector grid defined for the study area. During the image analysis process, the number of pixels belonging to the detected image segments was counted. Subsequently, a manual correction of the detected objects was conducted.

The total land area was defined as the total number of pixels in the analyzed orthophoto segment. Figure 3 illustrates an example of an orthophoto with segment boundaries and the resulting black-and-white mask.

(**a**) (**b**) (**c**)

Figure 3. Orthophoto (**a**) with segment boundaries (**b**) and the resulting black-and-white mask (**c**).

The recognition and marking of segments with green spaces was conducted via the web platform app.roboflow.com [22]. As a consequence of the operation of the neural network, the majority of the segments were identified successfully during the automatic recognition process. Subsequently, the manual refinement of the segmentation was conducted using the Smart Polygon tool [23].

2.3.2. Road Ratio (RR)

The road ratio is an important landscape indicator used in various fields such as urban planning, environmental studies, and landscape ecology. It provides insights into the degree of urbanization, accessibility, and the impact of transportation infrastructure on the landscape [24]. RR typically refers to the proportion of land area covered by roads relative to the total land area within a specific region or sector.

The RR can be calculated using GIS data by dividing the total area covered by roads by the total area of the region of interest (2). The formula is:

$$RR = \frac{Total\ Road\ Area}{Total\ Land\ Area} \times 100 \quad (2)$$

The total road area was calculated in GIS using the OpenStreetMap layer (Available online: https://www.openstreetmap.org/ (accessed on 8 September 2024)). OpenStreetMap was selected due to its detailed and up-to-date mapping of road networks, which is essential for the accurate calculation of RR [25]. It is known that all landscape elements in OpenStreetMap are marked with different colors. In particular, roads are marked with white, yellow, and orange colors depending on their traffic [26]. To calculate the total road area, all pixels of the OpenStreetMap layer segment corresponding to the road colors (white, yellow, and orange) were counted. The total land area was defined as the total number of pixels in the analyzed OpenStreetMap segment. An example of a map with roads highlighted is presented in Figure 4.

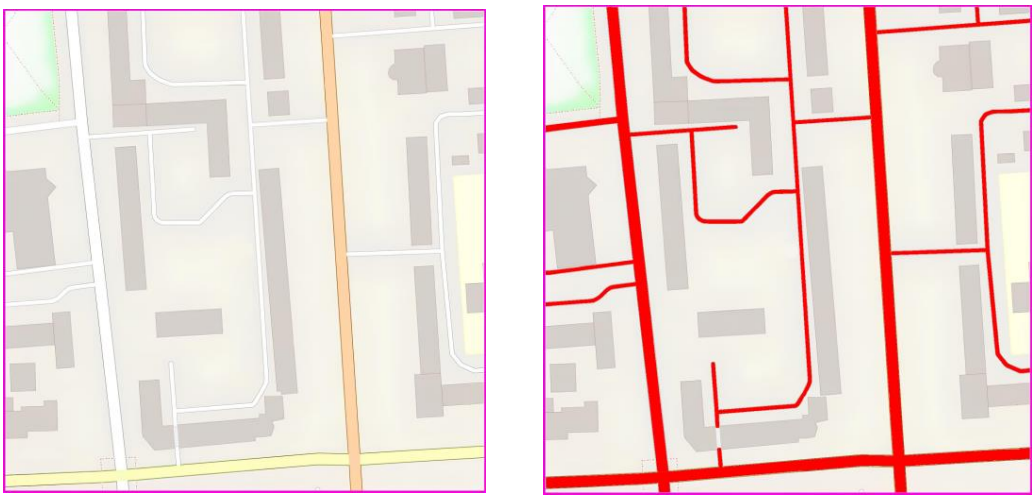

(**a**) (**b**)

Figure 4. Fragment of map from OpenStreetMap (**a**) with roads highlighted (**b**).

2.4. Air Quality Index (AQI)

The AQI is a numerical scale used to communicate how polluted the air currently is or how polluted it is forecast to become. It is an important tool for conveying the potential health effects of air pollution to the public. AQI is a critical measure that translates complex pollution data into a simple numerical scale, indicating the level of health concern due to air quality. The AQI focuses on health effects you may experience within a few hours or days after breathing polluted air [27]. The pollutants used to calculate AQI in this study include O_3, $PM_{2.5}$, PM_{10}, CO, SO_2, and NO_2.

The AQI is calculated based on the concentrations of various air pollutants. To calculate the AQI for each pollutant, standardized Formula (3) is used to convert pollutant

concentrations into an index value [28]. The highest AQI value among all pollutants is used to calculate the total AQI.

$$AQI = \frac{I_{high} - I_{low}}{C_{high} - C_{low}}(C - C_{low}) + I_{low} \quad (3)$$

where C is the measured concentration of the pollutant, C_{low} and C_{high} are the ranges of concentrations appropriate for this AQI category, and I_{low} and I_{high} are the ranges of AQI values for a given pollution level. The ranges for each pollutant that are used to determine AQI levels are presented in Table 2.

Table 2. Table of AQI categories and corresponding concentrations for major pollutants.

AQI Range	O_3 (ppm) * [28]	$PM_{2.5}$ (μg/m^3) ** [28,29]	PM_{10} (μg/m^3) ** [28,30]	CO (ppm) * [28]	SO_2 (ppb) *** [28]	NO_2 (ppb) *** [28]	Levels of Health Concern [28,30]
0–50	0.000–0.054	0.0–9.0	0–54	0.0–4.4	0–35	0–53	Good
51–100	0.055–0.070	9.1–35.4	55–154	4.5–9.4	36–75	54–100	Moderate
101–150	0.071–0.085	35.5–55.4	155–254	9.5–12.4	76–185	101–360	Unhealthy for Sensitive Groups
151–200	0.086–0.105	55.5–125.4	255–354	12.5–15.4	186–304	361–649	Unhealthy
201–300	0.106–0.200	125.5–225.4	355–424	15.5–30.4	305–604	650–1249	Very unhealthy
301–500	0.201–0.604 ****	225.5–325.4	425–604	30.5–50.4	605–1004	1250–2049	Hazardous

* 8 h average. ** 24 h average. *** 1 h average. **** 8-h O_3 values do not define higher AQI values (≥301). AQI values of 301 or higher are calculated using the AQI 500 limit for 1 h O_3 concentration.

2.5. Interpolations

In this study, the Multilevel b-spline interpolation (MLBS) method was employed to interpolate the data. MLBS proved to be a robust and versatile method for interpolating complex environmental datasets [31]. Its ability to capture both broad trends and fine details makes it an invaluable tool in the arsenal of numerical methods for scientific research [32]. MLBS was calculated using SAGA GIS v. 9.1.0 with the "Multilevel B-Spline" tool, cell size 50, scope West—8,562,112, South—6,843,819, East—8,574,562, North—6,856,769, threshold error 0.0001, and maximum level 9. The technique enabled the creation of high-resolution air quality maps, providing a detailed view of pollutant distributions. The accuracy and smoothness of the interpolated surfaces were crucial for identifying pollution hotspots and understanding spatial patterns in air quality data.

2.6. Statistical Analysis

2.6.1. Correlation Analysis

Correlation analysis was used to identify the degree of relationship between variables, which is crucial for understanding the mutual influence of various factors in the studied area. Both Pearson's and Spearman's correlation methods were initially considered. Pearson's method is used to determine the linear relationship between variables and is appropriate for normally distributed data. In contrast, Spearman's non-parametric method estimates monotonic dependence between variables, making it suitable for data that do not follow a normal distribution or contain outliers.

The analysis was performed using Python (v. 3.10.10) with libraries for scientific computing and statistical analysis such as Pandas (v. 2.2.2), NumPy (v. 2.0.1), and SciPy (v. 1.14.0). Heatmaps were generated using Matplotlib (v. 3.9.1) and Seaborn (v. 0.13.2) libraries to visualize the correlation matrices. These heatmaps graphically represent the degree of correlation between variables, with different color intensities indicating the strength and direction of the relationships.

Correlation analysis was conducted on both the entire dataset (integral) and across a grid of sectors (sectoral). For sectoral analysis, the mean value of the interpolated raster for each parameter within each sector's boundaries was used. This approach was necessary as indices like GSR and RR can only be calculated for specific territories, not for point data.

2.6.2. Structural Equation Modeling (SEM)

SEM was employed to analyze the factors affecting the AQI. The data were standardized using the StandardScaler method from the Scikit-learn library (v. 1.5.1), which brings all parameters to the same scale, potentially improving model convergence and interpretation.

In this analysis, the dependent variable was AQI, while the independent variables included air temperature, air humidity, pollutant concentrations, and geographic coordinates (latitude and longitude). The Semopy library (v. 2.3.11) was used to create and estimate the model parameters. The model estimation results included regression coefficients and statistical measures such as the value and significance of the coefficients.

2.6.3. Shapiro–Wilk Test

The Shapiro–Wilk test was employed to assess the normality of data distribution. This statistical method tests the null hypothesis that a sample comes from a normally distributed population. The test produces a *p*-value, which quantifies the evidence against the null hypothesis of normality. A *p*-value less than the chosen alpha level (0.05) suggests that the data significantly deviate from a normal distribution, leading to the rejection of the null hypothesis. The *p*-values for the Shapiro–Wilk test were calculated using the SciPy library (v. 1.14.0) in Python (v. 3.10.10), specifically the scipy.stats module.

2.6.4. Regression Analysis

Polynomial regression was utilized to analyze the relationship between AQI and the landscape indicators RR and GSR. Scatter plots were created to visualize the data distribution and assess potential patterns. Linear and quadratic regression models were fitted to both RR and GSR data to capture both linear and non-linear relationships. The choice of these models was based on initial exploratory data analysis and the assumption of potential non-linearity.

The coefficients of determination (R^2) were calculated for both models to assess their overall fit. The vertex of the quadratic curve was determined by finding the RR/GSR value associated with the minimum predicted AQI based on the model.

The required calculations were conducted using Python. Linear regression was performed using the np.polyfit function, while quadratic regression involved fitting a second-degree polynomial using the curve_fit function from scipy.optimize. The coefficients from these models were used to generate trend lines.

It is important to note that the analysis establishes correlations between AQI and the landscape indicators, but it does not imply causation. The identified relationships can provide insights for urban planning and environmental management but should be interpreted cautiously.

2.7. GIS and Mapping

The Geographic Information Systems (GISs) QGIS (v. 3.28.11) and SAGA GIS (v. 9.1.0) were used in this study. QGIS was applied to visualize, edit, and analyze spatial data, allowing geographic information to be processed and displayed efficiently. SAGA GIS was used to perform complex spatial analysis and modeling, including data interpolation. The combined use of these tools ensured the high accuracy and reliability of the results obtained.

During the study, OpenStreetMap, 2GIS maps, and Google satellite imagery were used for spatial analysis and data visualization in GIS. OpenStreetMap and 2GIS maps provided detailed information on the road network and infrastructure, while Google satellite imagery provided high-resolution and accurate landscape and land use data. The use of these data sources provided a comprehensive view of the study area and improved the accuracy of the spatial analysis.

3. Results

3.1. Descriptive Statistics of Data

Data on the concentrations of pollutants O_3, $PM_{2.5}$, PM_{10}, CO, SO_2, and NO_2 along with coordinates, air temperature, air humidity, and AQI calculated for every 713 observations are available in Supplementary Table S1. Descriptive statistics on the obtained dataset are presented in Table 3.

Table 3. Statistics on concentrations of pollutants and AQI values.

Pollutant	Mean	Median	Min	Max	Range	Std Dev	Q1	Q3	CV * (%)	Shapiro–Wilk Test *p*-Value
$PM_{2.5}$ (μg/m^3)	14.42	12.0	2.0	57.0	55.0	10.95	5.0	21.0	75.93	<0.001
PM_{10} (μg/m^3)	16.68	13.0	2.0	74.0	72.0	13.13	6.0	23.0	78.72	<0.001
CO (ppb)	979.51	873.0	<LOD **	4077	4077	534.95	596	1181	54.61	<0.001
SO_2 (ppb)	7.32	7.0	5.0	12.0	7.0	0.67	7.0	8.0	9.09	<0.001
NO_2 (ppb)	22.69	23.0	4.0	45.0	41.0	7.22	19.0	28.0	31.79	<0.001
O_3 (ppb)	28.73	29.0	10.0	46.0	36.0	6.11	25.0	34.0	21.26	<0.001
AQI	55.50	56.0	11.0	152.0	141.0	26.39	29.0	73.0	47.54	<0.001

* coefficient of variation. ** LOD—level of detection.

The analysis of data on pollutant concentrations and AQI in the study area shows significant variability of the parameters. The mean values of $PM_{2.5}$ and PM_{10} particulate matter concentrations are 14.42 μg/m^3 and 16.68 μg/m^3, respectively. These values are slightly higher than the median values (12.0 μg/m^3 for $PM_{2.5}$ and 13.0 μg/m^3 for PM_{10}), indicating that there are some high values in the sample. The standard deviation of these parameters is also quite high, indicating significant variability in the data. The coefficients of variation for $PM_{2.5}$ and PM_{10} are 75.93% and 78.72%, respectively, confirming the high variation of values around the mean.

CO concentrations range widely, from lower than LOD to 4077 ppb, with a mean of 979.51 ppb and a median of 873.0 ppb. This indicates wide variations in CO levels, which may be due to different emission sources or changes in environmental conditions. The standard deviation for CO is 534.95 ppb, and the coefficient of variation is 54.61%, which also indicates significant variability.

SO_2 shows the lowest variability among all measured parameters. The mean value of SO_2 concentration is 7.32 ppb, the median is 7.0 ppb, and the range of values is only 7.0 ppb. The low coefficient of variation of 9.10% indicates the ubiquity of SO_2 concentration, which may be the result of constant emission sources and relatively unchanged environmental conditions.

NO_2 concentrations have a mean of 22.69 ppb and a median of 23.0 ppb. The range of values is 41.0 ppb and the coefficient of variation is 31.80%, indicating moderate variability in the data. This may be due to different sources of NO_2 emissions such as transportation and industrial processes.

O_3 shows a mean value of 28.73 ppb and a median of 29.0 ppb, with a spread of 36.0 ppb and a coefficient of variation of 21.26%. These data indicate a relatively stable ozone concentration in the air, which may be related to constant photochemical reactions in the atmosphere.

The AQI has a mean of 55.50, a median of 56.0, and a spread of 141.0. The coefficient of variation for AQI is 47.55%, indicating that there is considerable variability in the index, reflecting overall air quality. This may be due to variations in the levels of various pollutants affecting air quality.

Very low *p*-values in the Shapiro–Wilk test indicate that the data obtained on concentrations of pollutants and AQI do not have a normal distribution.

3.2. Environmental Statistics

To identify the level of impact of pollutants on the environment, we compared the indicators of pollutant levels with the threshold values recommended by WHO in 2021.

The average daily recommended levels were used as thresholds (Table 4). For O_3, the threshold level corresponding to the 8 h average concentration was used. Additionally, AQI level was calculated for every point.

Table 4. Air quality guidelines (AQG) levels recommended by WHO for 2021 [33].

Pollutant	Averaging Time	2021 AQG Level
$PM_{2.5}$, $\mu g/m^3$	Annual	5
	24 h [a]	15
PM_{10}, $\mu g/m^3$	Annual	15
	24 h [a]	45
O_3, $\mu g/m^3$	Peak season [b]	60
	8 h [a]	100 (50.94 ppb)
NO_2, $\mu g/m^3$	Annual	10
	24 h [a]	25 (13.29 ppb)
SO_2, $\mu g/m^3$	24 h [a]	40 (15.28 ppb)
CO, mg/m^3	24 h [a]	4 (3491.61 ppb)

[a] Ninety-ninth percentile (i.e., 3–4 exceedance days per year). [b] Average of daily maximum 8 h mean O_3 concentration in the six consecutive months with the highest six-month running-average O_3 concentration.

Table 5 provides an analysis of pollutant concentrations, their respective threshold values, the threshold exceedance index, and the frequency of maximum AQI for every pollutant. For $PM_{2.5}$, the mean concentration is 14.42 $\mu g/m^3$, which is slightly below the threshold value of 15.00 $\mu g/m^3$. Despite this, the threshold exceedance index for $PM_{2.5}$ is relatively high at 39.83%, indicating that a significant portion of the measurements exceeds the threshold, reflecting frequent episodes of elevated $PM_{2.5}$ levels.

Table 5. Pollutant analysis: average concentrations, threshold values, and threshold exceedance index.

Pollutant	Mean	Threshold [33]	Threshold Exceedance Index, %	Frequency of Maximum AQI [a]
$PM_{2.5}$ ($\mu g/m^3$)	14.42	15.00	39.83	540 (75.7%)
PM_{10} ($\mu g/m^3$)	16.68	45.00	3.65	0
CO (ppb)	979.51	3491.61	0.56	0
SO_2 (ppb)	7.32	15.28	0.00	1 (0.1%)
NO_2 (ppb)	22.69	13.29	87.38	172 (24.1%)
O_3 (ppb)	28.73	50.94	0.00	0

[a] refers to the number of times a specific pollutant has been the primary contributor to AQI by having the highest individual AQI value among all measured pollutants.

PM_{10} shows a mean concentration of 16.68 $\mu g/m^3$, which is well below its threshold value of 45.00 $\mu g/m^3$. The threshold exceedance index for PM_{10} is low at 3.65%, suggesting that PM_{10} levels rarely exceed the threshold and are generally within safe limits.

For CO, the mean concentration is 979.51 ppb, much lower than the threshold value of 3491.61 ppb. The threshold exceedance index is very low at 0.56%, indicating that CO levels are typically within acceptable ranges and do not frequently pose a health risk.

SO_2 has a mean concentration of 7.32 ppb, which is below the threshold value of 15.28 ppb. The threshold exceedance index for SO_2 is 0.00%, showing that SO_2 levels are consistently within safe limits and do not exceed the threshold.

NO_2 presents a different scenario, with a mean concentration of 22.69 ppb, which exceeds the threshold value of 13.29 ppb. The threshold exceedance index is very high at 87.38%, indicating that NO_2 levels frequently surpass the threshold, suggesting a significant air quality concern for this pollutant.

O_3 has a mean concentration of 28.73 ppb, which is below its threshold value of 50.94 ppb. The threshold exceedance index for O_3 is 0.00%, indicating that ozone levels are consistently within safe limits and do not exceed the threshold.

Thus, the analysis highlights that while most pollutants like PM_{10}, CO, SO_2, and O_3 are generally within safe limits, there are significant concerns with $PM_{2.5}$ and particularly NO_2, which frequently exceed their respective threshold values, indicating potential health risks and the need for targeted air quality management strategies.

Since the AQI is equal to the maximum value of all individual AQIs, it is important to identify the pollutants that have the greatest impact on this index. This can be performed by calculating how many times each pollutant has reached the maximum AQI value. Table 5 shows that $PM_{2.5}$ and NO_2 contributed the most to the formation of the AQI level, exhibiting maximum individual AQI for 75.7% and 24.1% of the points, respectively.

The categorical distribution of AQI values is presented in Figure 5. The air quality in the study area can be characterized as follows: out of 713 surveyed points, in 300 points (42.08%), the air is of "good" quality. This means that in a significant part of the study area at the sampling moment, the air was safe for all categories of people without posing health risks.

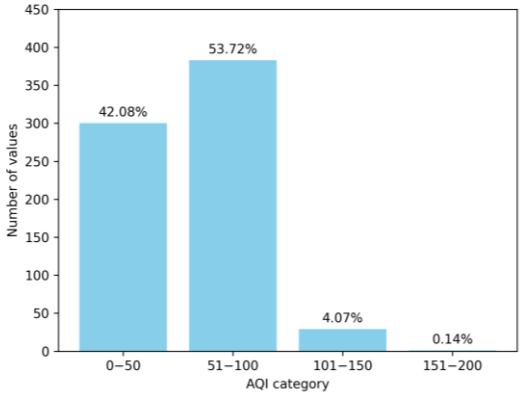

Figure 5. Distribution of AQI Values.

In 383 points (53.72%), the air quality is moderate. This means that the air is still relatively safe in most locations, but people with sensitive systems such as children, the elderly, or people with respiratory conditions may experience minor discomfort. Despite this, moderate air quality is still within acceptable standards and does not cause serious problems for most of the population.

There are also a small number of points, precisely 29 (4.07%), where air quality is harmful to sensitive populations. In these locations, people with asthma, allergies, or other chronic diseases may experience worsening health conditions and should take extra precautions. These locations require special attention and possible intervention to minimize exposure to sensitive populations.

Additionally, one point (0.14%) with harmful air quality was recorded. In such locations, most people may experience negative effects from air pollution, especially sensitive groups, although this figure is very small and may relate to random emissions in the data.

Thus, air quality in the study area can be considered mostly good to moderate (95.8% of points), which is a positive indicator. Nevertheless, the presence of points with harmful air quality (4.21%) emphasizes the importance of regular monitoring and taking measures to improve air quality to protect the health of the population, especially vulnerable groups.

3.3. Results of the Landscape Indicators Calculation

To define the influence of landscape indicators on the air quality and pollutant levels, the GSR and RR indices were calculated for every sector of the grid that intersects or lies within the boundaries of the research area. Moreover, interpolation rasters were obtained for every pollutant, and the mean value of concentrations was calculated for every sector. Such sectoral analysis makes it possible to include GSR and RR indices in statistical analyses.

After calculation, the database on the sectors was obtained (Supplementary Table S2). Every parameter was calculated for 347 sectors, so the total area of sectors included achieved 31.23 km^2. The average GSR is 23.4%, which corresponds to a total greenery area of 7.31 km^2. The average RR is 4.75%, corresponding to a total road coverage area of 1.48 km^2. The relation of GSR/RR is 4.9.

3.4. Results of Correlation Analysis

3.4.1. Sectoral Correlation Analysis

Sectoral analysis was conducted to identify correlations between the urban landscape indices, pollutants, and AQI within specific city sectors, as illustrated in the Spearman correlation chart with *p*-values (Figure 6). Notably, GSR showed weak negative correlations with PM_{10}, $PM_{2.5}$, $SO_{2,}$ and AQI, indicating that an increase in green space is weakly associated with a decrease in pollutant concentrations and an improvement in air quality. These correlations were statistically significant, with *p*-values close to zero.

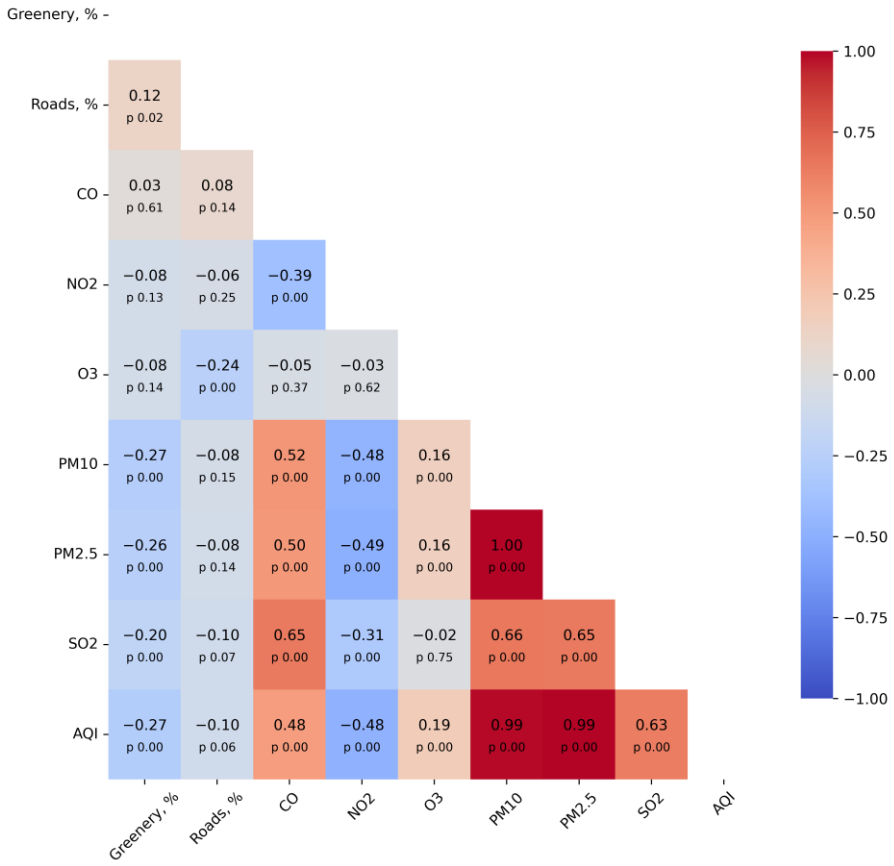

Figure 6. Spearman correlation between urban landscape indices, air pollutants, and AQI with significance (*p*-values) based on sectoral analysis.

RR shows a weak negative correlation with O_3 levels, indicating that an increase in the road-coated area is associated with a decrease in ground-level O_3 concentration. Other correlations of RR were not statistically significant with the *p*-values above 0.05.

CO concentration has a moderate negative correlation with NO_2; a stronger positive correlation with PM_{10}, $PM_{2.5}$, and AQI; and a significant positive correlation with SO_2, indicating that these pollutants are often found together. These correlations are also statistically significant.

NO_2 concentration shows a negative correlation with PM_{10}, $PM_{2.5}$, SO_2, CO, and AQI, suggesting that a decrease in NO_2 levels is associated with an increase in overall air pollu-

tion. NO_2 appears to have independent sources. Ozone concentration has a weak negative correlation with $PM_{2.5}$ and PM_{10}, but these relationships are not statistically significant.

PM_{10} and $PM_{2.5}$ concentrations show a high positive correlation with each other and with AQI, which is expected since both are major components affecting the air quality index. A very high positive correlation between $PM_{2.5}$ and PM_{10} suggests that they often coexist and likely share common sources. AQI also shows a moderate positive correlation with CO, and SO_2, indicating that these pollutants significantly impact overall air quality.

In conclusion, the analysis reveals that major pollutants such as PM_{10}, $PM_{2.5}$, and SO_2 have a significant impact on the air quality index. Importantly, the study suggests that increasing green space can potentially improve air quality by reducing the concentration of these pollutants. These findings have important implications for urban planning and environmental management strategies aimed at improving air quality in cities.

3.4.2. Integral Correlation Analysis

The integral correlation analysis consolidates data from all observation points within the study area, enabling the identification of correlations between pollutant concentration levels at each point, AQI, geographical coordinates, and air humidity and temperature parameters. The corresponding Spearman correlation coefficients with *p*-values are shown in Table 6.

Table 6. Spearman correlation between air conditions, pollutants, geographical coordinates, and AQI with significance (*p*-values) based on integral analysis.

Pollutant	Humidity	Temperature	Y Coordinate (Latitude)	X Coordinate (Longitude)
AQI	0.63 $p = 0.00$	−0.37 $p = 0.00$	0.28 $p = 0.00$	0.72 $p = 0.00$
$PM_{2.5}$	0.65 $p = 0.00$	−0.39 $p = 0.00$	0.30 $p = 0.00$	0.72 $p = 0.00$
PM_{10}	0.62 $p = 0.00$	−0.36 $p = 0.00$	0.30 $p = 0.00$	0.73 $p = 0.00$
CO	0.15 $p = 0.00$	0.06 $p = 0.13$	0.37 $p = 0.00$	0.41 $p = 0.00$
SO_2	0.21 $p = 0.00$	0.04 $p = 0.29$	0.40 $p = 0.00$	0.51 $p = 0.00$
NO_2	−0.52 $p = 0.00$	0.35 $p = 0.00$	−0.14 $p = 0.00$	−0.30 $p = 0.00$
O_3	0.40 $p = 0.00$	−0.27 $p = 0.00$	−0.29 $p = 0.00$	0.11 $p = 0.00$

Air humidity shows a moderate positive correlation with $PM_{2.5}$ and PM_{10} concentrations, meaning that higher humidity levels are associated with higher concentrations of these pollutants. Air humidity also shows a moderate negative correlation with NO_2, suggesting that higher NO_2 levels are associated with lower humidity.

According to the observations, air temperature shows a weak negative correlation with AQI, and this correlation is statistically significant. However, it is reasonable to conclude that the exact cause of this correlation cannot be determined with absolute accuracy without long-term temporal studies.

The strongest correlations were observed between the X coordinate and AQI, $PM_{2.5}$, and PM_{10} levels. The correlation is strongly positive, suggesting an increase in pollution levels in the eastern direction. Additionally, the Y coordinates weakly positively correlate with pollutants and AQI. These correlations suggest a potential influence of geographical location on pollutant distribution. The correlations of coordinates indicate a trend of increasing AQI in the east-northeast direction. This trend correlates with areas influenced by industrial zones. The periphery of the urban area in proximity to industrial zones exhibits a distinct industrial landscape, with an abundance of construction sites, repair

shops, garages, vehicle depots, and other facilities that have the potential to be a source of dust pollution. Additionally, these zones tend to be less subjected to greening than residential areas within the city.

Notably, during the sampling period, the wind direction was predominantly from the southwest (Figure 7), which should have mitigated the influence from the industrial area by carrying air masses away from the residential zone towards the industrial sector. The wind directions observed during the study period generally corresponded to the average historical wind rose diagram (Figure 8). However, despite the favorable wind direction from the residential zone towards the industrial area, zones with elevated concentrations of particulate matter were identified within the residential sector. These areas were adjacent to the industrial zones. Therefore, it can be inferred that the influence of the industrial sector could increase significantly under opposite wind conditions.

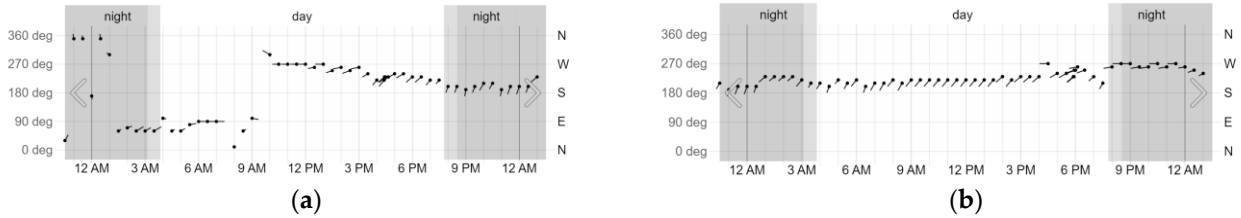

Figure 7. Wind directions for Pavlodar city specified to sampling period: (**a**) 19 May 2024; (**b**) 20 May 2024 measured at Pavlodar Airport at approximately 10 m above an open field. Civil twilight and night are indicated by shaded overlays [34].

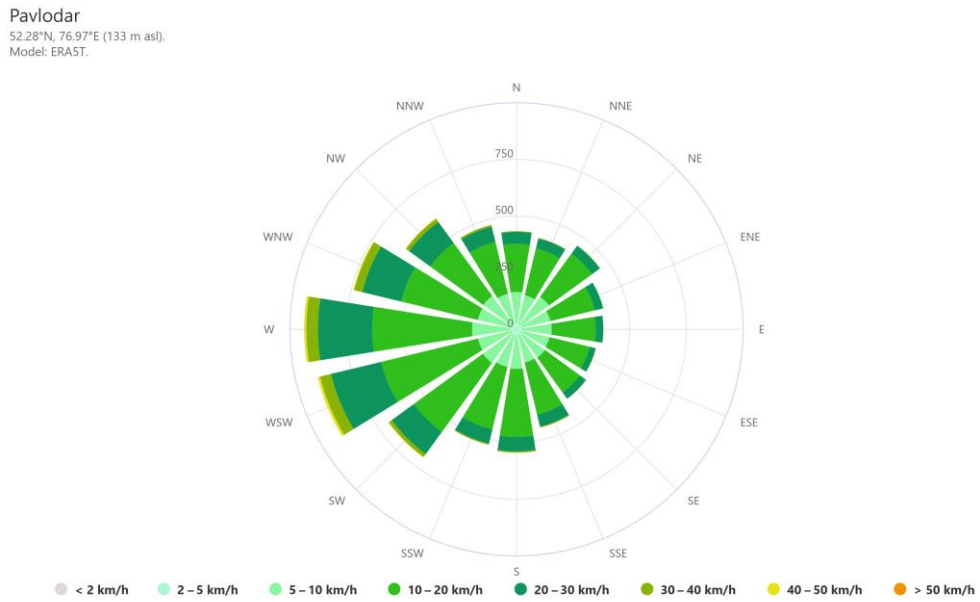

Figure 8. Average historical (from 1940 till now) wind rose diagram for Pavlodar city [35].

These findings highlight the complex interplay between geographical factors, urban development, and air quality, emphasizing the need for comprehensive urban planning strategies that consider both industrial activities and green space distribution.

3.5. SEM Analysis

This study employed SEM to examine relationships between environmental factors and AQI. The results of the integral path analysis using SEM are presented in Table 7.

Table 7. Integral path analysis results from the structural equation model: effects of environmental factors on air quality index (AQI).

Dependent Variable	Relation	Independent Variable	Estimate	Std. Error	z-Value	*p*-Value
AQI	→	Air Temperature	0.097	0.013	7.639	2.18×10^{-14}
AQI	→	Air Humidity	0.250	0.017	14.885	$<1.00 \times 10^{-16}$
AQI	→	$PM_{2.5}$	0.949	0.038	25.093	$<1.00 \times 10^{-16}$
AQI	→	PM_{10}	−0.076	0.035	−2.150	3.16×10^{-2}
AQI	→	CO	0.005	0.006	0.766	4.44×10^{-1}
AQI	→	SO_2	−0.033	0.006	−5.205	1.94×10^{-7}
AQI	→	NO_2	0.039	0.006	6.518	7.12×10^{-11}
AQI	→	O_3	0.024	0.006	3.915	9.05×10^{-5}
AQI	→	Latitude	−0.012	0.005	−2.328	1.99×10^{-2}
AQI	→	Longitude	0.013	0.007	1.780	7.51×10^{-2}
AQI	↔	AQI	0.014	0.001	18.881	$<1.00 \times 10^{-16}$

The integral analysis showed that $PM_{2.5}$ demonstrated the most substantial positive impact on AQI, underscoring its critical role in air pollution. According to the low *p*-value, this influence is statistically significant. Unlike correlation analysis, SEM analysis allows us to specify not only correlations but also the more complex influence of independent factors on the dependent variable, in our case AQI. Using this method, we were able to exclude the significant influence of pollutants such as PM_{10} and NO_2.

3.6. Regression Analysis for the Relationship between AQI and Landscape Indicators

The scatter plot analysis of AQI versus GSR reveals a complex relationship between urban greenery and air quality (Figure 9). Linear regression yields $y = -0.5013x + 70.4744$ ($R^2 = 0.0697$), indicating a weak negative correlation, as in correlation analysis. Both parameters (slope, intercept) in the linear function are characterized by low *p*-values (0.000 for both parameters), which indicates that they are highly statistically significant.

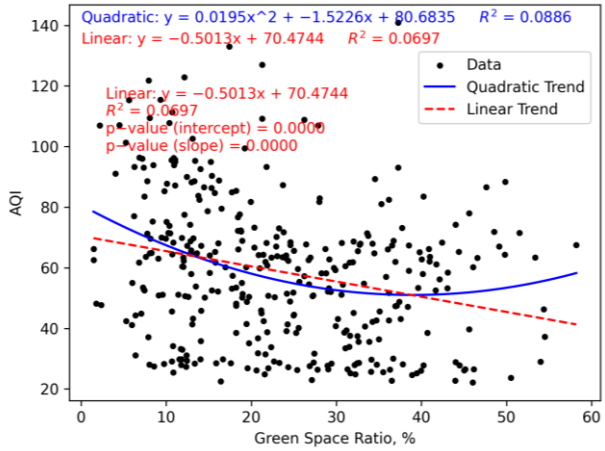

Figure 9. Relationship between AQI and GSR (%).

The quadratic model, $y = 0.0195x^2 - 1.5226x + 80.6835$ ($R^2 = 0.0886$), provides a slightly better fit, suggesting a non-linear relationship. We calculated the *p*-values for the coefficients and the constant of the quadratic regression. The *p*-value for a (the x^2 term) is 0.00787, the *p*-value for b (the x term) is 0.00013, and the *p*-value for c (the constant term) is 0.00000. Thus, all three coefficients are less than 0.05 and are therefore statistically significant at the standard significance level of 5%. This indicates that the components of the quadratic model have a significant impact on the dependent variable.

The quadratic curve's vertex (GSR ≈ 38.98%, AQI ≈ 51.01) represents an optimal green space threshold for minimizing AQI. Beyond this point, further increases in GSR correlate

with a slight AQI increase. While both models exhibit low R^2 values, signifying substantial unexplained variability, they nonetheless provide valuable insights. The analysis suggests that increasing green space by up to approximately 39% may improve air quality, after which benefits diminish. These findings underscore the importance of balanced urban green space planning for optimal air quality outcomes, while also highlighting the need for the consideration of additional factors influencing urban air quality in future research.

The relationship between the AQI and RR is illustrated in Figure 10. Linear regression analysis yields an equation of $y = -1.4858x + 65.8067$ with an R^2 value of 0.0169, indicating a weak negative correlation between AQI and increasing road coverage. Slope and intercept coefficients in the linear function are characterized by low *p*-values (0.0154 and 0.000 correspondingly), which indicates that they are highly statistically significant.

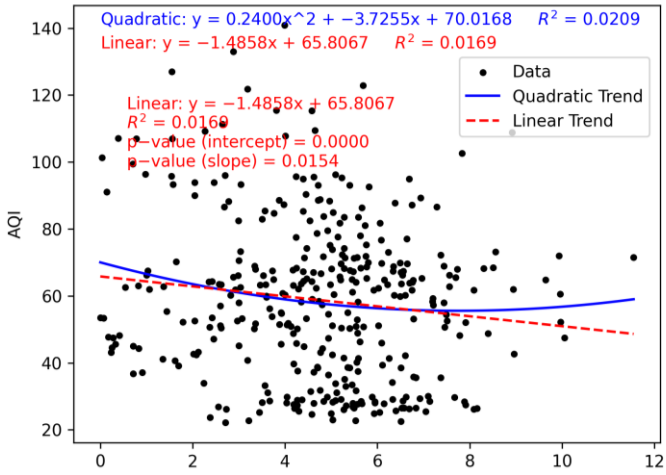

Figure 10. Relationship between AQI and RR (%).

A quadratic model, described by the equation $y = 0.2400x^2 - 3.7255x + 70.0168$ with an R^2 of 0.0209, demonstrates an improved fit to the data, albeit still representing a weak relationship. The *p*-value for a (the x^2 term) is 0.23828, the *p*-value for b (the x term) is 0.06225, and the *p*-value for c (the constant term) is 0.00000. The coefficients *a* and *b* in the model are not statistically significant, especially *a* (quadratic component), which has a *p*-value well above the threshold of 0.05. The coefficient *b* (linear component) also does not reach the standard level of significance, although it is close to it.

Thus, AQI and RR are rather poorly correlated, which is reflected in both the correlation analysis results and the regression analysis calculations. The low R^2 values for both models (1.69% and 2.09%, respectively) indicate that the RR accounts for only a small fraction of the variance in AQI. This underscores the necessity of considering additional variables to achieve more accurate air quality predictions.

3.7. Spatial Analysis of AQI Distribution in Pavlodar

During the research, two maps presenting the spatial distribution of AQI in the residential area of Pavlodar city were obtained, utilizing different classification methods to visualize air quality patterns (Figure 11).

In the map (Figure 11), the AQI was classified using equal intervals, providing a more nuanced view of air quality variations across the study area. The color scheme ranges from blue (representing the lowest AQI values of ≤35) through green, yellow, orange, and red (indicating the highest AQI values of >136). This classification reveals a complex spatial pattern of air quality within the city. The western and central parts of the study area show predominantly lower AQI values, represented by blue and green hues, suggesting better air quality in these regions. In contrast, the eastern and southeastern portions of the map display higher AQI values, indicated by yellow, orange, and red colors, pointing to areas with potentially poorer air quality.

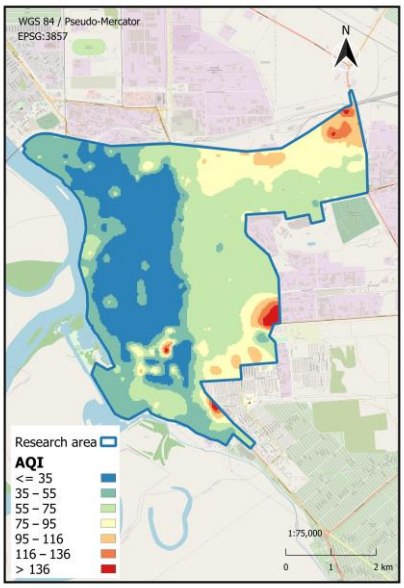

Figure 11. Spatial distribution of AQI in the residential area of the Pavlodar city classified with equal intervals.

The spatial patterns revealed by this map could be valuable for urban planning, environmental management, and public health initiatives in Pavlodar. They identify areas where air quality improvement measures might be most needed and could guide the placement of additional air quality monitoring stations. Table 8 provides a breakdown of AQI values from the MLBS interpolation raster categorized by health concern levels, along with the count and percentage of observations within each range.

Table 8. Frequency distribution of the AQI values in Pavlodar from an interpolated raster of the research area classified according to the AQI scale defined by the US-EPA 2016 standard [36].

AQI Range	Levels of Health Concern	Pixel Count	Percentage, %
0–50	Good	11,439	39.01
51–100	Moderate	16,728	57.05
101–150	Unhealthy for Sensitive Groups	1145	3.90
151–200	Unhealthy	11	0.04
201–300	Very unhealthy	0	0.0

The majority of AQI values fall within the "Good" and "Moderate" categories. The "Good" category (AQI 0–50) includes 11,439 pixels, accounting for 39.01% of observations, indicating generally favorable air quality with little health risk. The "Moderate" category (AQI 51–100) has 16,728 pixels, or 57.05%, suggesting acceptable air quality with a slight concern for sensitive individuals. This is the most common AQI range, indicating mostly moderate air quality in Pavlodar.

The "Unhealthy for Sensitive Groups" category (AQI 101–150) comprises 1145 pixels (3.90%), indicating potential health effects for sensitive groups, though the general public is less affected. The "Unhealthy" category (AQI 151–200) is rare, with only 11 pixels (0.04%), posing a risk to all, especially sensitive groups. There are no points in the "Very Unhealthy" category (AQI 201–300), indicating no instances of severely poor air quality.

Given the positive correlation between AQI and $PM_{2.5}$ and PM_{10}, it can be confidently assumed that the spatial distribution of AQI will largely correspond to that of particulate matter. Conversely, NO_2 concentration demonstrated an inverse correlation with AQI, indicating that the spatial distribution of this pollutant will be different. Figure 12 illustrates that exceeding the threshold level of NO_2 is rather permanent and exhibits no pronounced

spatial trends. This distribution pattern suggests that motor vehicles are the primary source of nitrogen dioxide, rather than industrial sources.

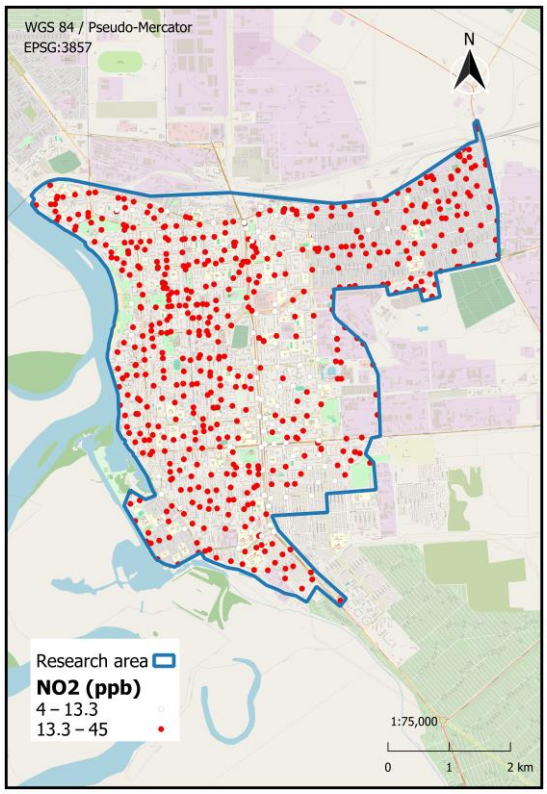

Figure 12. Spatial distribution of NO_2 in the residential area of Pavlodar city, highlighting the points exceeding the WHO-AQG thresholds.

Overall, the data suggests that Pavlodar experiences predominantly "moderate" air quality, with very few instances of unhealthy air conditions. This distribution highlights the city's generally favorable environmental conditions while also identifying the need for continued monitoring and efforts to maintain or improve air quality to protect public health.

4. Discussion

The study identified $PM_{2.5}$ and NO_2 as the main contributors to air pollution in the study area. In particular, NO_2 exceeded the 24 h threshold in 87.38% of locations, whereas $PM_{2.5}$ had the highest individual AQI in 75.7% of cases, underscoring its dominant influence. This observation is supported by the correlation analysis, which shows a positive correlation between $PM_{2.5}$ and AQI. Additionally, a negative correlation was identified between NO_2 and AQI. This inverse relationship is probably due to the overshadowing effect of $PM_{2.5}$; in areas exhibiting elevated $PM_{2.5}$ levels, NO_2 concentrations tend to decline while the AQI rises, as the AQI is predominantly influenced by $PM_{2.5}$. This dynamic is due to the AQI calculation method, which prioritizes the dominant pollutant.

To further clarify these interactions, the SEM analysis shows that $PM_{2.5}$ has the most significant impact on AQI (0.95), while NO_2 has no significant correlation or negative impact. The strong correlation between $PM_{2.5}$ and PM_{10} suggests common sources. In general, pollutants such as CO, O_3, PM_{10}, $PM_{2.5}$, and SO_2 demonstrate a positive correlation with the AQI, indicating that an increase in their concentrations is associated with an elevation of the AQI level. However, NO_2 deviates from this pattern. Although it frequently exceeds daily thresholds, its negative correlation with $PM_{2.5}$ diminishes its direct effect on AQI, as shown in the analysis.

Humidity positively correlated with AQI, so an increase in humidity increased the AQI. It is also important to note that this correlation between AQI and humidity does

not necessarily imply a strict or universal relationship. This correlation is observed only for the period of observations (May) and should be interpreted within this context. The relationship can be explained by seasonal weather patterns typical for this month, such as decreasing temperatures before rain, accompanied by increasing wind speeds. These conditions can lead to the more active movement of dust particles, temporarily affecting air quality. Therefore, while the data show a correlation, it may not represent a causal relationship between humidity and AQI that holds across all seasons or locations.

The landscape indices GSR and RR were examined within a sectoral analysis. GSR shows a weak negative correlation with AQI and the main pollutants (except CO). Statistically significant correlations were found between GSR and $PM_{2.5}$, PM_{10}, SO_2, and AQI. However, the correlations were weak, indicating that while green spaces positively impact air quality, this influence is not strong. This is consistent with the literature, which suggests that vegetation can reduce airborne pollutants through deposition and absorption [37–39]. However, a strong relationship is difficult to demonstrate due to urban trees being planted in various locations, including more polluted areas. Additionally, the planting density is insufficient to notably reduce pollutant levels, resulting in only a minimal difference between sectors with high and low GSR. Nevertheless, regression analysis revealed a statistically significant minimum in the quadratic trend at 39%, indicating that, despite statistical challenges, an increase in green space till the threshold level leads to a reduction in pollution.

Unlike GSR, RR does not provide sufficient statistical evidence to draw conclusions about its impact on air quality. This negative result may be due to the study's methodology, which measured road surface area rather than traffic intensity. Given the small size of the studied city, the road surface area often does not correlate with traffic intensity [40], which is a major determinant of urban air pollution.

It is noteworthy that GSR and RR show a weak positive correlation (0.12, p-value = 0.02), likely due to the approaches in urban greenery, with a significant portion planted along roads for protective purposes [41].

The study's findings indicate significant spatial variability in concentrations of pollutants such as $PM_{2.5}$, PM_{10}, CO, SO_2, NO_2, and O_3 across Pavlodar city. Integral correlation analysis revealed a strong positive correlation between the X coordinate and a moderate positive correlation between the Y coordinate and pollutants $PM_{2.5}$, PM_{10}, and AQI. This spatial distribution corresponds to increasing pollution levels toward the east-northeast, likely influenced by the Northern Industrial Zone and the northern part of the Eastern Industrial Zone. The spatial analysis shows a correlation between AQI and the proximity to industrial zone boundaries, despite the opposite wind direction during the sampling. This indicates the negative impact of industrial activity on the atmosphere in residential areas adjacent to industrial zones. This outcome is expected given the presence of major industrial facilities with extensive industrial territories, including railroads, construction sites, warehouses, and garages. These findings are consistent with previous research highlighting the significant contribution of industrial activities to urban air pollution [15,42,43]. The main possible sources for the studied pollutants are vehicle and industrial emissions, road dust, and industrial processes.

In contrast, nitrogen dioxide pollution does not exhibit a discernible correlation with geographic coordinates. This conclusion is supported by both correlation analysis and the map of the spatial distribution of exceedances of NO_2 thresholds. The observed distribution of this pollutant suggests that vehicles represent its primary source.

The spatial interpolation of air quality data using the Multilevel B-Spline method identified distinct pollution hotspots, particularly in areas adjacent to major industrial and traffic zones. These hotspots pose significant public health risks, especially for vulnerable populations such as children, the elderly, and individuals with pre-existing respiratory conditions. The central and western parts of the city are the least affected by pollution. The peripheral distribution of pollutants and the low incidence of pollution hotspots in

residential areas indicate that the primary sources of pollution, including particulate matter, are industrial sites located in industrial zones.

Overall, the air quality in Pavlodar at the time of the study was classified as "moderate" according to AQI levels. However, the observed levels of pollutants, particularly $PM_{2.5}$ and NO_2, exceeded WHO guidelines in a significant number of points, necessitating urgent policy interventions, even though the WHO guidelines do not provide any classification for levels of health risk [44,45].

Based on the findings, several policy measures are recommended to improve air quality in Pavlodar city:

1. Expansion of Green Spaces: Increasing urban green spaces can significantly reduce air pollution and enhance the overall environmental quality. Initiatives such as creating urban parks, green roofs, and tree planting, especially in industrial zones and along the edges of the residential area, should be prioritized.
2. Industrial Emission Controls: Strengthening regulations on industrial emissions and encouraging the adoption of cleaner technologies can reduce the release of harmful pollutants from industrial activities.
3. Public Awareness and Engagement: Raising public awareness about the sources and health impacts of air pollution and engaging communities in air quality management efforts can foster collective action towards a cleaner environment. Equally important is the development of the practice of regular air quality monitoring by consolidating private and public monitoring stations in a single network.

The implementation of the proposed recommendations is crucial for both residents and visitors of industrialized cities. Air quality plays a pivotal role in determining the quality of life in urban areas. For instance, Pavlodar, the city analyzed in this study, is not only an industrial center but also holds significant cultural value, including a high tourism potential. Pavlodar is a destination for business, ecological, and cultural tourism [16,46,47]. However, polluted air not only poses a risk to the health of residents but also diminishes the city's appeal to tourists seeking a healthy and comfortable environment. In this context, up-to-date information on the atmospheric conditions in residential areas is essential for the sustainable development of tourist infrastructure, such as hotels and parks, in regions with better air quality. Therefore, regular monitoring and the development of methods for assessing the ecological state of urban air are not only vital for enhancing tourist satisfaction but also support the sustainable development of the city. Improving air quality through the collaboration of residents, industry, and urban management is critical not only for public health protection but also for boosting the city's tourism potential, which in turn contributes to economic growth and sustainability.

The findings of this study have broader implications beyond air quality management, particularly in the areas of tourism-related infrastructure, transport, and logistics. The identified spatial variability in pollutant concentrations and the pollution hotspots near industrial zones provide critical insights for planning and developing sustainable urban infrastructure. By integrating pollution data into urban planning, cities can develop more efficient and environmentally friendly transportation systems that minimize exposure to pollutants [48,49]. The expansion of green spaces can serve a dual purpose: improving air quality and creating an attractive, healthy environment that enhances the city's tourism appeal and provides logistical advantages by improving urban aesthetics and reducing the heat island effect [50].

This article contributes to the development of methods for improving air quality management in industrial cities by offering tailored solutions for specific areas, taking into account their unique environmental and industrial characteristics. These methods assist local administrators and urban planning specialists in better understanding the complexity of interactions between industrial zones, green spaces, and air quality, as well as in identifying the most effective environmental and infrastructure measures. Additionally, the study's findings emphasize the importance of regular air quality monitoring and mapping to support urban planning and transportation infrastructure development decisions aimed at

reducing pollution levels. In conclusion, this research advances approaches for integrating green infrastructures with technological and industrial solutions, which is a key factor in designing sustainable and environmentally friendly cities.

While this study provides valuable insights into the spatial distribution of air pollutants and their determinants, it has several limitations. The short duration of data collection may not fully capture temporal variations in pollutant levels. Certain limitations are associated with the method of air quality analysis. Thus, it is not possible to obtain data on a sufficiently large number of points simultaneously. Monitoring covering the whole city area takes considerable time and can last up to two days. During this period, local concentrations may change. However, general trends and correlations should remain quite reliable. In addition, monitoring in different seasons could be helpful for a better understanding of the peculiarities of air pollution in the city.

Despite the use of the road ratio index, it was not possible to measure the traffic intensity in different sectors of the city, which could significantly contribute to the analysis of pollution pathways.

Future research should focus on long-term monitoring to better understand temporal trends and the effectiveness of implemented policies. Integrating additional data sources, such as satellite observations and citizen science contributions, can also enhance the robustness of air quality assessments.

5. Conclusions

In conclusion, this research provides valuable insights into the spatial distribution of air pollutants in Pavlodar city, highlighting the significant impact of industrial activities and vehicular emissions on air quality. The study found that $PM_{2.5}$ and NO_2 are the primary pollutants influencing AQI, as well as NO_2 frequently exceeding the WHO's recommended thresholds. There is a notable correlation between higher GSR and lower AQI levels, suggesting that urban green spaces play a crucial role in mitigating air pollution. The study reveals significant spatial variability in pollutant concentrations across Pavlodar city, with increasing pollution levels toward the east-northeast, likely due to the industrial landscape and activity that brings pollutants from industrial zones to residential areas.

Pavlodar faces significant environmental challenges as an industrial hub, with high pollutant concentrations adversely affecting public health and quality of life. The data indicate predominantly "moderate" air quality according to the AQI level, but further long-term monitoring is needed to capture seasonal variations. The study recommends several policy measures to improve air quality, including expanding green spaces, strengthening industrial emission controls, and raising public awareness about air pollution and its health impacts. Integrating public and private air quality monitoring networks is also highlighted as essential for comprehensive management.

This research underscores the importance of addressing air quality not only as a public health concern but also as a critical factor in the sustainable development of urban infrastructure, tourism, and logistics. The spatial analysis of pollutants provides valuable data that can be used to optimize the location of tourism-related infrastructure, ensuring that such developments contribute to a healthier urban environment. Additionally, the findings suggest that strategic urban planning, which includes the expansion of green spaces and the careful routing of transport networks, can significantly contribute to reducing pollution levels. By incorporating these environmental considerations, cities can enhance their sustainability, improve public health outcomes, and create a more attractive environment for both residents and visitors. The integration of air quality data into urban planning, particularly in industrial cities, is essential for developing infrastructure that supports economic growth while safeguarding environmental and public health.

Supplementary Materials: The following supporting information can be downloaded at https://www.mdpi.com/article/10.3390/su16177834/s1. Table S1: Integral monitoring data; Table S2: Sectoral monitoring data.

Author Contributions: Conceptualization, R.S.; methodology, R.S.; software, R.K.; validation, E.K.; formal analysis, Y.N.; investigation, Y.N.; resources, R.K.; data curation, Z.S.; writing—original draft, R.S.; writing—review and editing, E.K.; visualization, Z.B.; supervision, Z.S.; project administration, R.S.; funding acquisition, R.S. All authors have read and agreed to the published version of the manuscript.

Funding: This research was funded by the Science Committee of the Ministry of Science and Higher Education of the Republic of Kazakhstan within the framework of the grant AP19677560 "Monitoring and mapping of the ecological state of the Pavlodar air environment using machine learning methods".

Institutional Review Board Statement: Not applicable.

Informed Consent Statement: Not applicable.

Data Availability Statement: Data is contained within the article or Supplementary Material.

Acknowledgments: We would like to thank Kuanysh T. Kydralin, the Head of the Department of Education of Pavlodar at the Administration of Education of Pavlodar region, for outstanding collaboration in organizing air quality monitoring within the framework of this research.

Conflicts of Interest: The authors declare no conflicts of interest. The funders had no role in the design of the study; in the collection, analyses, or interpretation of data; in the writing of the manuscript; or in the decision to publish the results.

References

1. Health Consequences of Air Pollution. Available online: https://www.who.int/news/item/25-06-2024-what-are-health-consequences-of-air-pollution-on-populations (accessed on 26 June 2024).
2. Kasimgaliev, S.; Kelinbaeva, R.; Sultanov, M.; Zhunisbekova, N. Geoinformation Support, Analysis, Evaluation and Forecasting of the Use of Land Resources of Kyzylorda Region. *Bull. LN Gumilyov Eurasian Natl. Univ. Chem. Geogr. Ecol. Ser.* **2023**, *144*, 105–118. [CrossRef]
3. Seidaliyeva, A.; Kabdushev, S.; Baipakbayeva, S.; Kopishev, E.; Suleimenov, I. The Diversification of Energy Sources in Kazakhstan as a Way to Dampen the Consequences of a Predicted Crisis. *Polityka Energ.* **2024**, *27*, 173–188. [CrossRef]
4. Menconi, M.; Abbate, R.; Simone, L.; Grohmann, D. Urban Green System Planning Insights for a Spatialized Balance between PM10 Dust Retention Capacity of Trees and Urban Vehicular PM10 Emissions. *Sustainability* **2023**, *15*, 5888. [CrossRef]
5. Wang, T.; Zhang, F.; Gu, H.; Hu, H.; Kaur, M. A Research Study on New Energy Brand Users Based on Principal Component Analysis (PCA) and Fusion Target Planning Model for Sustainable Environment of Smart Cities. *Sustain. Energy Technol. Assess.* **2023**, *57*, 103262. [CrossRef]
6. Zaini, N.; Ahmed, A.N.; Ean, L.W.; Chow, M.F.; Malek, M.A. Forecasting of Fine Particulate Matter Based on LSTM and Optimization Algorithm. *J. Clean. Prod.* **2023**, *427*, 139233. [CrossRef]
7. Zhangarasheva, G.K.; Zhaksalykova, G.B.; Kenesova, A.A.; Sarmanov, A.A.; Shaikhiev, S.S.; Makashev, D.M. *The Health of the Population of the Republic of Kazakhstan and the Activities of Healthcare Organizations in 2020. Statistical Digest*; Ministry of Health of the Republic of Kazakhstan: Nur-Sultan, Kazakhstan, 2021; p. 324.
8. Eusébio, C.; Rodrigues, V.; Carneiro, M.J.; Madaleno, M.; Robaina, M.; Monteiro, A. The Role of Air Quality for Reaching Tourism Environmental Sustainability: A Segmentation Approach Based on Visitors' pro-Environmental Behaviors. *Int. J. Tour. Res.* **2023**, *25*, 455–473. [CrossRef]
9. Sharma, S.; Jain, S.; Khirwadkar, P.; Kulkarni, S. The Effects of Air Pollution on the Environment and Human Health. *Indian J. Res. Pharm. Biotechnol.* **2013**, *3*, 391–396.
10. Kaur, J.; Jhamaria, C. Urban Air Pollution and Human Health: A Review. *Curr. World Environ.* **2021**, *16*, 362–377. [CrossRef]
11. Vinnikov, D.; Tulekov, Z.; Raushanova, A. Occupational Exposure to Particulate Matter from Air Pollution in the Outdoor Workplaces in Almaty during the Cold Season. *PLoS ONE* **2020**, *15*, e0227447. [CrossRef]
12. Amouei Torkmahalleh, M.; Kabay, K.; Bazhanova, M.; Mohiuddin, O.; Obaidullah, M.; Gorjinezhad, S. Investigating the Impact of Different Sport Trainings on Particulate Matter Resuspension in a Sport Center Using Well-Characterized Reference Instruments and a Low-Cost Monitor. *Sci. Total Environ.* **2018**, *612*, 957–965. [CrossRef]
13. Kerimray, A.; Azbanbayev, E.; Kenessov, B.; Plotitsyn, P.; Alimbayeva, D.; Karaca, F. Spatiotemporal Variations and Contributing Factors of Air Pollutants in Almaty, Kazakhstan. *Aerosol Air Qual. Res.* **2020**, *20*, 1340–1352. [CrossRef]
14. Kerimray, A.; Bakdolotov, A.; Sarbassov, Y.; Inglezakis, V.; Poulopoulos, S. Air Pollution in Astana: Analysis of Recent Trends and Air Quality Monitoring System. *Mater. Today Proc.* **2018**, *5*, 22749–22758. [CrossRef]
15. Safarov, R.Z.; Shomanova, Z.K.; Kopishev, E.E.; Nossenko, Y.G.; Bexeitova, Z.B. Spatial Distribution of PM2.5 and PM10 Pollutants in Residential Area of Pavlodar, Kazakhstan. *News Natl. Acad. Sci. Repub. Kazakhstan-Ser. Chem. Technol.* **2023**, *457*, 181–200. [CrossRef]
16. Isiksal, A.Z.; Isiksal, H.; Zhakanovna, R.S.; Sagatbayevna, S.A.; Zhakanov, A. Ecological Development Impact on Tourism in Pavlodar Region. *Economics* **2018**, *6*, 113–124. [CrossRef]

17. Alimbaev, T.; Khassenova, Z.; Zhalmurzina, A. The Environmental State of the Pavlodar Region in the Republic of Kazakhstan (1990s). *E3S Web Conf.* **2024**, *510*, 03034. [CrossRef]
18. Kanibolotskaya, Y.; Listkov, W.; Shmidt, N. Heavy Metals in Soil and Plants (Agropyron Pectiniforme Roem. et Schult.) of the Pavlodar Region (Kazakhstan). In Proceedings of the International Conference on Sustainable Development of Cross-Border Regions, Barnaul, Russia, 19–20 April 2019; IOP Publishing: Bristol, UK, 2019; Volume 395, p. 012037.
19. Davidenko, L.; Sherimova, N.; Kunyazova, S.; Amirova, M.; Beisembina, A. Sustainable Economy: The Eco-Branding of an Industrial Region in Kazakhstan. *Sustainability* **2024**, *16*, 413. [CrossRef]
20. Annerstedt Van Den Bosch, M.; Mudu, P.; Uscila, V.; Barrdahl, M.; Kulinkina, A.; Staatsen, B.; Swart, W.; Kruize, H.; Zurlyte, I.; Egorov, A.I. Development of an Urban Green Space Indicator and the Public Health Rationale. *Scand. J. Public Health* **2016**, *44*, 159–167. [CrossRef]
21. YOLOv8: A New State-of-the-Art Computer Vision Model. Available online: https://yolov8.com/ (accessed on 22 June 2024).
22. Roboflow. Available online: https://app.roboflow.com/ruslan-safarov-bbfgy/city-vxbsv/visualize/7 (accessed on 21 June 2024).
23. Lynn, T. Launch: Smart Polygon Labeling. Available online: https://blog.roboflow.com/automated-polygon-labeling-computer-vision/ (accessed on 21 June 2024).
24. Martín, B.; Ortega, E.; Otero, I.; Arce, R.M. Landscape Character Assessment with GIS Using Map-Based Indicators and Photographs in the Relationship between Landscape and Roads. *J. Environ. Manag.* **2016**, *180*, 324–334. [CrossRef]
25. OpenStreetMap. Available online: https://www.openstreetmap.org/ (accessed on 22 June 2024).
26. Map Features—OpenStreetMap Wiki. Available online: https://wiki.openstreetmap.org/wiki/Map_features (accessed on 22 June 2024).
27. AQI Basics | AirNow.Gov. Available online: https://www.airnow.gov/aqi/aqi-basics (accessed on 22 June 2024).
28. Technical Assistance Document for the Reporting of Daily Air Quality. Available online: https://www.airnow.gov/publications/air-quality-index/technical-assistance-document-for-reporting-the-daily-aqi/ (accessed on 22 June 2024).
29. US EPA, O. Final Reconsideration of the National Ambient Air Quality Standards for Particulate Matter (PM). Available online: https://www.epa.gov/pm-pollution/final-reconsideration-national-ambient-air-quality-standards-particulate-matter-pm (accessed on 22 June 2024).
30. Wambebe, N.M.; Duan, X. Air Quality Levels and Health Risk Assessment of Particulate Matters in Abuja Municipal Area, Nigeria. *Atmosphere* **2020**, *11*, 817. [CrossRef]
31. Safarov, R.; Shomanova, Z.; Nossenko, Y.; Mussayev, Z.; Shomanova, A. Digital Visualization of Environmental Risk Indicators in the Territory of the Urban Industrial Zone. *Sustainability* **2024**, *16*, 5190. [CrossRef]
32. Lee, S.; Wolberg, G.; Shin, S.Y. Scattered Data Interpolation with Multilevel B-Splines. *IEEE Trans. Vis. Comput. Graph.* **1997**, *3*, 228–244. [CrossRef]
33. World Health Organization. *WHO Global Air Quality Guidelines: Particulate Matter (PM2.5 and PM10), Ozone, Nitrogen Dioxide, Sulfur Dioxide and Carbon Monoxide*; WHO: Geneva, Switzerland, 2021.
34. May 20, 2024 Historical Weather at Pavlodar Airport, Kazakhstan—Weather Spark. Available online: https://weatherspark.com/h/d/149003/2024/5/20/Historical-Weather-on-Monday-May-20-2024-at-Pavlodar-Airport-Kazakhstan#Sections-WindDirection (accessed on 30 August 2024).
35. Simulated Historical Climate & Weather Data for Pavlodar. Available online: https://www.meteoblue.com/en/weather/historyclimate/climatemodelled/pavlodar_kazakhstan_1520240 (accessed on 6 August 2024).
36. Air Quality Index Scale and Color Legend. Available online: https://aqicn.org/scale/ (accessed on 25 June 2024).
37. Yan, J.; Chen, W.Y.; Zhang, Z.; Zhao, W.; Liu, M.; Yin, S. Mitigating PM2.5 Exposure with Vegetation Barrier and Building Designs in Urban Open-Road Environments Based on Numerical Simulations. *Landsc. Urban Plan.* **2024**, *241*, 104918. [CrossRef]
38. Yuan, Y.; Zhou, P.; Peng, M.; Zhu, L.; Li, Y.; Wang, K.; Wang, Y.; Tang, Z.; Wang, Y.; Huang, Y.; et al. Residential Greenness Mitigates Mortality Risk from Short-Term Airborne Particulate Exposure: An Individual-Level Case-Crossover Study. *Ecotoxicol. Environ. Saf.* **2023**, *264*, 115451. [CrossRef]
39. Sadyrova, G.; Tanybayeva, A.; Bazarbaeva, T.; Mukanova, G.; Jamilova, S.; Nurmakhanova, A. Analysis of the Ecological State of Urban Green Spaces in the Medeu District of Almaty. *Bull. LN Gumilyov Eurasian Natl. Univ. Chem. Geogr. Ecol. Ser.* **2023**, *145*, 83–92. [CrossRef]
40. Geng, L.; Zhang, K. Correlation of Road Network Structure and Urban Mobility Intensity: An Exploratory Study Using Geo-Tagged Tweets. *ISPRS Int. J. Geo-Inf.* **2023**, *12*, 7. [CrossRef]
41. Mori, J.; Fini, A.; Galimberti, M.; Ginepro, M.; Burchi, G.; Massa, D.; Ferrini, F. Air Pollution Deposition on a Roadside Vegetation Barrier in a Mediterranean Environment: Combined Effect of Evergreen Shrub Species and Planting Density. *Sci. Total Environ.* **2018**, *643*, 725–737. [CrossRef]
42. Guo, D.; Wang, R.; Zhao, P. Spatial Distribution and Source Contributions of PM2.5 Concentrations in Jincheng, China. *Atmos. Pollut. Res.* **2020**, *11*, 1281–1289. [CrossRef]
43. Patiño-Aroca, M.; Hernández-Paredes, T.; Panchana-López, C.; Borge, R. Source Apportionment of Ambient Pollution Levels in Guayaquil, Ecuador. *Heliyon* **2024**, *10*, e31613. [CrossRef]
44. Franke, P.; Lange, A.C.; Steffens, B.; Pozzer, A.; Wahner, A.; Kiendler-Scharr, A. European Air Quality in View of the WHO 2021 Guideline Levels: Effect of Emission Reductions on Air Pollution Exposure. *Elementa* **2024**, *12*, 00127. [CrossRef]
45. Burki, T. WHO Introduces Ambitious New Air Quality Guidelines. *Lancet* **2021**, *398*, 1117. [CrossRef]

46. Yessim, A.; Shokhan, R.; Yessimova, D.; Faurat, A.; Safarov, R.; Sonko, S.M. Analysis of the Economic State of the Tourist Industry in the Pavlodar Region (Kazakhstan). *Geoj. Tour. Geosites* **2023**, *47*, 596–604. [CrossRef]
47. Yessimova, D.; Faurat, A.; Belyy, A.; Yessim, A.; Novikova, A.; Olshanskaya, M.; Safarov, R.; Bilalov, B.; Bumbak, S.-V. Assessment of the Readiness of the Tourism Industry in the Pavlodar Region for the Implementation of Sustainable Tourism. *Geoj. Tour. Geosites* **2024**, *54*, 967–976. [CrossRef]
48. Feng, Z.; Zeng, X.; Li, W. Revealing Urban Traffic Emission Patterns: A Complex Network Perspective. *Energy Proc.* **2024**, *47*. [CrossRef]
49. Elgohary, A.S.; Samra, M.; El-Madawy, A.E.-T. Sustainable Urban Treatments for Mixed-Use (Residential-Industrial) Areas in Egypt (Fuwah Case Study). *Civ. Eng. Archit.* **2024**, *12*, 1124–1142. [CrossRef]
50. Picone, N.; Esposito, A.; Emmanuel, R.; Buccolieri, R. Potential Impacts of Green Infrastructure on NOx and PM10 in Different Local Climate Zones of Brindisi, Italy. *Sustainability* **2024**, *16*, 229. [CrossRef]